The Brightness Temperatures of the Main Galactic Radio-Loops at 22 MHz

D. Urošević[1,*] and V. Borka Jovanović[2]

[1]*Department of Astronomy, Faculty of Mathematics, University of Belgrade, Studentski trg 16, 11000 Belgrade, Serbia*
[2]*Atomic Physics Laboratory (040), Vinća Institute of Nuclear Sciences, University of Belgrade, P. O. Box 522, 11001 Belgrade, Serbia*

Abstract: The average brightness temperatures and surface brightnesses at 22 MHz are derived for the four main Galactic radio-continuum loops (Loops I, II, III and IV, hereafter radio-loops). Also the radio-continuum spectra for the radio-loops are presented. Adding the average brightness temperatures at 22 MHz derived here with the average brightness temperatures derived from spectra published previously at 408, 820 and 1420 MHz we obtained clearly non-thermal spectral indices for all radio-loops. Our derived spectral indices are slightly shallower than those measured by previous works.

Keywords: Radiation mechanisms, non-thermal, radio continuum, general, surveys.

1. INTRODUCTION

The radio-spurs are angularly immense and clearly visible features on the radio-sky[1]. It is known that sets of radio-spurs which form small circles on the celestial sphere are called radio-loops. Four major Galactic radio-continuum loops were recognized as Loops I - IV (see [2]). Their origin is probably from local supernova explosions. They are probably very old (a few million years) supernova remnants (bubbles) or superbubbles originated in one or several supernova explosions, respectively. A detailed review of the subject was published in [3].

In order to study the origin of emission from the radio loops, it is necessary to determine their spectral indices. The spectral indices of the radio-loops by using radio-continuum surveys at three frequencies: 1420 MHz [4], 820 MHz [5] and 408 MHz [6], were studied in [7], where then calculated the corresponding mean temperatures and brightnesses. Until [7] and [8] papers there were no spectra obtained by using mean temperatures for (at least) two different frequencies, which is necessary for obtaining the simplest linear spectrum. All earlier determinations of the radio loop spectral indices were based on TT methods[2].

In this paper we derive the average brightness temperatures and surface brightnesses of the radio-loops from the radio-continuum survey at 22 MHz [9] and construct the new spectra of radio-loops using data at the four different frequencies (1420, 820, 408, and 22 MHz).

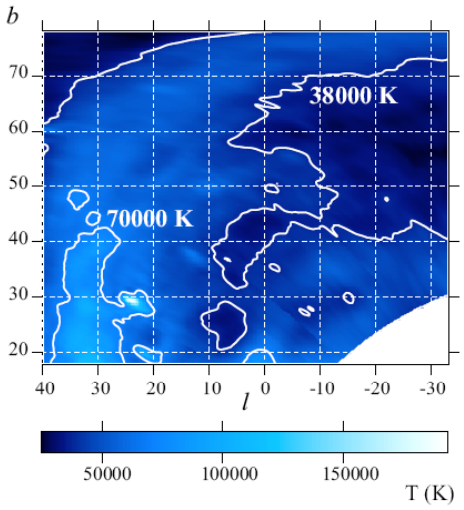

Fig. (1). Left: temperature scales for 22 MHz. It is given in K and they are used for all figures of the radio-loops given below. Right: the area of Loop I at 22 MHz, showing contours of brightness temperature. This contains the part of the North Polar Spur (NPS) normal to the Galactic equator: l = [40., 0.]; b = [18., 78.], and its part parallel to the Galactic equator: l = [360., 327.]; b = [67., 78.]. Two contours are plotted, those representing the temperatures T_{min} and T_{max}, as given in Table **1**.

2. ANALYSIS

The data were obtained from the 22 MHz survey conducted with the Dominion Radio Astrophysical Observatory (DRAO) [9]. The angular resolution is 1.1° x 1.7°. The effective sensitivity is about 500 K. The telescope comprises seven 9-m equatorially-mounted paraboloids on

*Address correspondence to this author at the Department of Astronomy, Faculty of Mathematics, University of Belgrade, Studentski trg 16, 11000 Belgrade, Serbia; Tel: +381 11 20 27 827; Fax: +381 11 2 630 151;
E-mail: dejanu@math.rs

[1]The angular diameter of Loop I is approximately 120° [1].

[2]The differential spectral index for the extended radio object can be derived from measurements at two different radio frequencies, when the brightness temperatures are plotted at the so-called temperature -- temperature (T-T) graph.

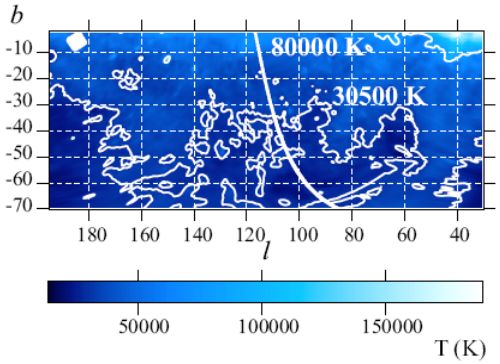

Fig. (2). The area of Loop II at 22 MHz, showing contours of brightness temperature. The two contours plotted represent the temperatures T_{min} and T_{max}, as given in Table **1**. The white area and white curved line in the figure mean that no data exist there at that frequency. Spurs belonging to this radio-loop have positions: l = [57., 30.], b = [-50., -10.] for spur in Aquarius and l = [195., 130.], b = [-70., -2.] for spur in Aries.

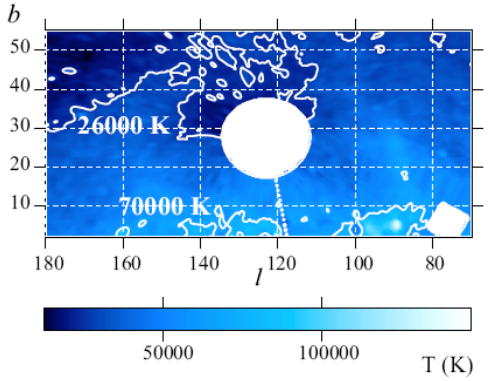

Fig. (3). The area of Loop III at 22 MHz, showing contours of brightness temperature. The two contours plotted represent the temperatures T_{min} and T_{max}, as given in Table **1**. The white area in the figure means that no data exist there at that frequency. Spurs belonging to this radio-loop have positions: l = [180., 135.]; b = [2., 50.] and l = [135., 110.]; b = [40., 55.] for the first spur and l = [110., 70.]; b = [6., 50.] for the second one.

an east-west line 600 m in extent. These data are available on MPIfR's Survey Sampler ('Max-Planck-Institut für Radioastronomie', Bonn). This is an online service (http://www.mpifrbonn.mpg.de/survey.html), which allows users to pick a region of the sky and obtain images at a number of wavelengths.

The areas of the loops were divided into different sections (corresponding to spurs), and these sections were combined for the final calculation of average brightness temperature a loop (see Figs. (**1**-**4**)). The longitude and latitude ranges which include spurs of the Loops I - IV are given in Table **1**. Background radiation was subtracted in the following manner: first, the temperature of the loop plus background was determined; next, the background alone immediately near the loop was estimated (Fig. (**5**)); finally, we calculated the difference of these values to yield the average temperature of the loop.

The contour lines, which correspond to the minimum and maximum brightness temperatures for each spur, are taken to

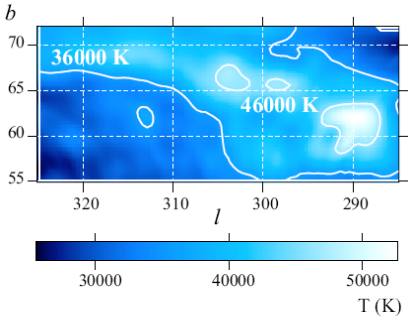

Fig. (4). The area of Loop IV at 22 MHz, showing contours of brightness temperature. The two contours plotted represent the temperatures T_{min} and T_{max}, as given in Table **1**. This radio-spur has position: l = [330., 290.]; b = [48., 70.].

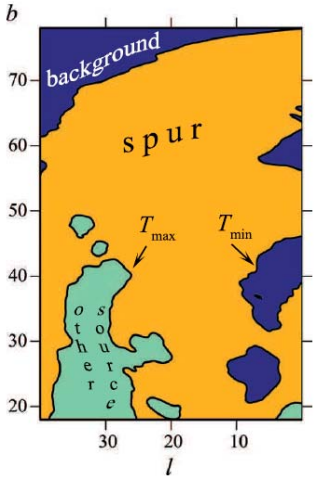

Fig. (5). The section of NPS from which data are sampled.

define their borders. T_{min} is the lower temperature limit between the background and the spur, and T_{max} is the upper temperature limit between the spur and unrelated confusing sources (superimposed on the spur and hence requiring elimination from the calculation). In this manner, background radiation was considered as radiation that would exist if there were no spurs. We used averages over the data within these two curves: the contour for T_{min} and the contour for T_{max}. More details are given in [7].

For evaluating brightness temperatures of the background, we used all measured values below T_{min}, inside the corresponding intervals of Galactic longitude (l) and Galactic latitude (b), and lying on the outer side of a spur (Fig. (**5**)). For evaluating the brightness temperatures of a loop including the background, we used all measured values between T_{min} and T_{max} inside the corresponding regions of l and b. Mean brightness temperatures for spurs are found by subtracting the mean values of background brightness temperature from the mean values of the brightness temperature over the areas of the spurs. For more details about the method see [7].

Table 1. The Galactic Longitude and Latitude for Spurs Belonging to Loops I — IV and the Lower and Upper Temperature Limits for These Loops at 22 MHz

Object	l Interval ($^\circ$)	b Interval ($^\circ$)	T_{min} (K)	T_{max} (K)
Loop I	l = [40, 0]	b = [18, 78]	38000	70000
	l = [360, 327]	b = [67, 78]		
Loop II	l = [57, 30]	b = [-50, -10]	30500	80000
	l = [195, 130]	b = [-70, -2]		
Loop III	l = [180, 135]	b = [2, 50]	26000	70000
	l = [135, 110]	b = [40, 55]		
	l = [110, 70]	b = [6, 50]		
Loop IV	l = [325, 285]	b = [55, 72]	36000	46000

Table 2. Brightness Temperatures (K), Surface Brightnesses Σ ($10^{-22}\ W\ m^{-2}\ Hz^{-1}\ sr^{-1}$) and Spectral Indices β ($T_b \propto \nu^{-\beta}$) Derived in this Paper. For Comparison, in the Last Two Columns are given the Spectral Indices and the Surface Brightnesses from [7] Borka (2007) (Signed by B07)

Object	$T_{22\,MHz}$	$\Sigma_{22\,MHz}$	β	$\Sigma_{1000\,MHz}$	β (B07)	$\Sigma_{1000\,MHz}$ (B07)
Loop I	17600 ± 500	26.8 ± 0.8	2.64 ± 0.03	2.4 ± 0.6	2.74 ± 0.08	2.3 ± 0.7
Loop II	12100 ± 500	18.3 ± 0.8	2.60 ± 0.06	2.1 ± 0.7	2.88 ± 0.03	1.9 ± 0.5
Loop III	18000 ± 500	27.3 ± 0.8	2.63 ± 0.02	2.4 ± 0.6	2.68 ± 0.06	2.4 ± 0.6
Loop IV	9400 ± 500	14.2 ± 0.8	2.77 ± 0.06	0.8 ± 0.6	2.90 ± 0.30	0.8 ± 0.7

Generally, our estimates of the average brightness temperatures of loops could be overestimated if the background temperatures have some gradient.

3. RESULTS

The results for the radio-loops obtained in this paper are presented in Table **2**, which lists the calculated average brightness temperatures and surface brightnesses at 22 MHz, spectral indices calculated using all, available average brightness temperatures at 1420, 820, 408, and 22 MHz. The last column in Table **2** shows the surface brightness Σ at 1000 MHz calculated using the spectral indices from third column in Table **2**. The surface brightnesses at 1000 MHz are calculated for comparison with earlier results. When comparing results at 1000 MHz derived here with values calculated earlier the good agreement of these results is obvious (see [7] and references therein), and expected since the measurement at 22 MHz is far from 1000 MHz to have any effect.

Spectra of the radio-loops are presented in Figs. (**6**-**9**). If we compare the spectral indices (defined by the relation $T \propto \nu^{-\beta}$) derived here with spectral indices derived in [7] the slightly shallower slopes are derived in this paper ($\Delta\beta \approx 0.1$, see Table **2**). The radio-spectra of many astrophysical objects have turnover near frequency of 100 MHz. The environment becomes optically thick at low frequencies and due to this physical condition, slope of the spectrum becomes opposite in its orientation at the frequencies below turnover frequency. Anyway, we observed the result of this effect as absorption in continuum (also it can be synchrotron selfabsorption) in the low frequency part of radio-spectrum. The measurements of surface brightness at 22 MHz could be below the maximal surface brightness that should probably be near 100 MHz. Since we added to the spectra the low frequency points at 22 MHz, the shallower spectrum should be expected. The shallower spectral indices obtained in this paper (Table **2**) should be used with caution -- the spectral indices obtained earlier (with the data at higher frequencies) should be preferable used for description of the synchrotron emission originated from radio-loops. For eventual identification of spectral turnover, the average surface brightnesses of the radio-loops between 22 and 408 MHz are needed.

4. CONCLUSIONS

i) In this paper, we have calculated the average brightness temperatures and surface brightnesses of the radio-loops at 22 MHz.

ii) The values of spectral indices that we derived are slightly shallower (but clearly non-thermal) than the values obtained in Borka (2007). It should be expected effect because we added to the spectra low frequency points at 22 MHz.

iii) We present the first radio-continuum spectra for the radio-loops using average brightness temperatures at four different frequencies.

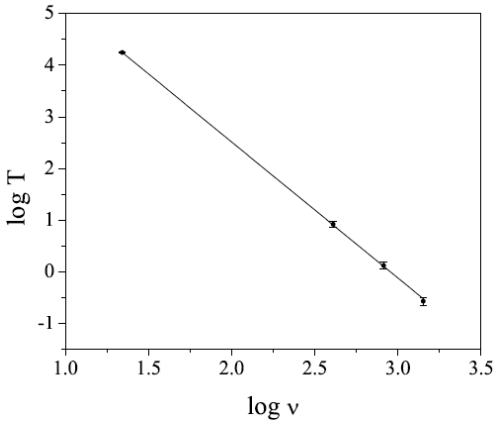

Fig. (6). The spectrum of Loop I: $\log T(\log \nu)$ for four measurements – at 22, 408, 820 and 1420 MHz. Relative errors of the measurements $\Delta \log T = \Delta T T \ln 10$ are presented by error bars, where ΔT are the corresponding absolute errors given in Table **2**.

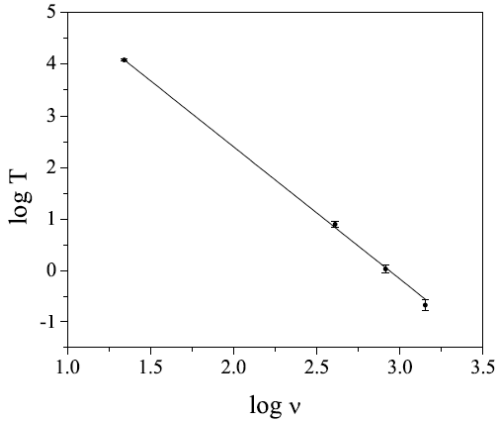

Fig. (7). The same as in Fig. (**5**), but for Loop II.

CONFLICIT OF INTEREST

None declared.

ACKNOWLEDGEMENT

We would like to thank the referee and handling editor for valuable comments. This work is part of the projects 176005 "Emission nebulae: structure and evolution" and 176003 "Gravitation and the large scale structure of the Universe" supported by the Ministry of Education and Science of Serbia.

REFERENCES

[1] Milogradov-Turin J, Urošević D. Geometry of large radio loops at 1420 MHz. Bull Astron Belgrade 1997; 155: 41.

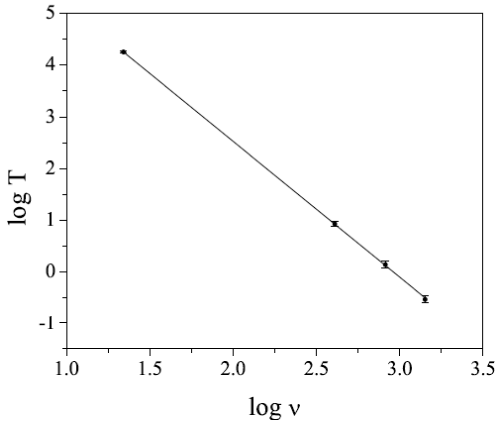

Fig. (8). The same as in Fig. (**5**), but for Loop III.

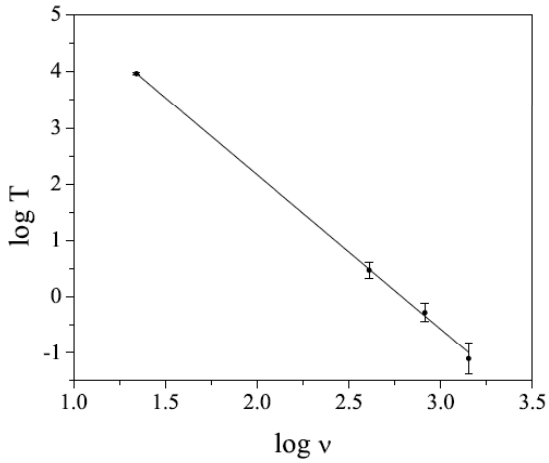

Fig. (9). The same as in Fig. (**5**), but for Loop IV.

[2] Berkhuijsen EM, Haslam CGT, Salter CJ. Are the galactic loops supernova remnants? Astron Astrophys 1971; 14: 252.

[3] Salter CJ. Loop-I the north polar spur - a major feature of the local interstellar environment. Bull Astron Soc India 1983; 11: 1.

[4] Reich P, Reich WA. Radio continuum survey of the northern sky at 1420 MHz. II. Astron Astrophys Suppl Ser 1986; 63: 205.

[5] Berkhuijsen EM. A survey of the continuum radiation at 820 MHz between declinations -7° and +85°. I. Observations and reductions. Astron Astrophys Suppl Ser 1972; 5: 263.

[6] Haslam CGT, Salter CJ, Stoffel H, Wilson WE. A 408 MHz all-sky continuum survey. II - The atlas of contour maps. Astron Astrophys Suppl Series 1982; 47: 1.

[7] Borka V. Spectral indices of Galactic radio loops between 1420, 820 and 408 MHz. Mon Not R Astron Soc 2007; 376: 634.

[8] Borka V, Milogradov-Turin J, Urošević D. The brightness of the galactic radio loops at 1420 MHz: Some indications for the existence of Loops V and VI. Astron Nachr 2008; 329: 397.

[9] Roger RS, Costain CH, Landecker TL, Swerdlyk CM. The radio emission from the Galaxy at 22 MHz. Astron Astrophys Suppl Ser 1999; 137: 7.

Received: May 24, 2011 Revised: August 04, 2011 Accepted: August 13, 2011